Benchmarking Phase Filtering Techniques for Coherence Enhancement and Persistent Scatterer Selection in PSInSAR

Pamungkas Y.A. [1,2*], Chiang S.H.[1]

[1]Center for Space and Remote Sensing Research, National Central University, Taiwan

[2]Department of Urban and Regional Planning, Universitas Brawijaya, Indonesia

*yanakhbarp@ub.ac.id

Abstract: *The accuracy of Persistent Scatterer Interferometric Synthetic Aperture Radar (PSInSAR) relies on effective coherence estimation to identify optimal Persistent Scatterer Point Candidates (PSCs). This study aims to evaluate and compare the performance of various phase filtering techniques, namely Boxcar, Goldstein, GAMMA, and Lee Filtering, with no filtering as the baseline, to compute the Spatial and Temporal Coherence for PSCs selection. A total of 173 Sentinel 1A Single Look Complex (SLC) images in ascending orbit with IW2 subswath and VV polarization images over Jakarta Capital City, Indonesia, were used. The processing workflow is composed of orbit correction, coregistration, wrapped interferogram generation, coherence estimation, and PSCs mask generation under different filtering scenarios. The results demonstrate significant variations in coherence performance among phase filtering methods, with spatial coherence consistently outperforming temporal coherence (spatial mean: 0.41 – 0.76; temporal mean: 0.07 – 0.12). GAMMA filtering yields the highest spatial coherence (mean = 0.76), indicating its superior ability to suppress speckle while preserving coherent signals in urban environments. In contrast, the no-filter scenario produces the lowest coherence values, highlighting the essential role of filtering in PSInSAR processing. Goldstein and Lee filters deliver reduced spatial coherence (means = 0.42 and 0.46), resulting in less detail and lower accuracy in persistent scatterer identification. Notably, Boxcar filtering achieves a spatial coherence (mean = 0.72) comparable to GAMMA, suggesting selective coherence preservation but with potential trade-offs in spatial detail. These findings underscore the critical influence of filter selection on the quality of coherence computation and have significant implications for enhancing PSInSAR accuracy in urban deformation studies. Future work will focus on comparing the results with unwrapped and cleaned phase as the input, as well as mapping the spatial distribution of stable scatterers through coherence thresholding and relating their occurrence to specific land cover types, providing deeper physical insight into the filtering results.*

Keywords: Coherence Estimation, Persistent Scatterer, Phase Filtering, PSInSAR, Sentinel-1

Introduction

Persistent Scatterer Interferometric Synthetic Aperture Radar (PSInSAR) has become a reliable remote sensing technique extensively utilized for monitoring land surface deformation, particularly in urban areas experiencing subsidence or structural instability (Ferretti et al., 2001; Hooper, 2008). The accuracy of PSInSAR-derived deformation measurement is critical, as errors or inaccuracies directly affect the interpretation of deformation patterns and the subsequent decision-making process (Hanssen, 2001; Wu & Madson, 2024). Measurement inaccuracies can arise from various sources, including atmospheric disturbances, orbital uncertainties, temporal decorrelation, and inherent noise

within SAR phase data (Zebker & Villasenor, 1992). Mitigating these errors through improved coherence estimation techniques is vital for reliable deformation measurement.

A fundamental step in achieving accurate deformation measurement through PSInSAR is the identification and selection of reliable Persistent Scatterer Candidates (PSCs). PSCs are points exhibiting stable scattering characteristics over time, typically corresponding to buildings, infrastructures, or naturally stable reflectors (Ferretti et al., 2001). Phase-based coherence indices, namely Temporal Coherence (Hooper et al., 2004) and Spatial Coherence (Zebker & Villasenor, 1992), are widely employed for this purpose. Temporal coherence assesses the phase stability of individual scatterers over the temporal series, while spatial coherence evaluates the consistency of the scatterer phase signal with neighboring pixels. Efficient PSCs selection based on these indices significantly enhances the robustness and accuracy of PSInSAR-derived deformation maps.

However, wrapped interferograms generated during SAR processing inherently contain noise from various sources, such as speckle, atmospheric phase delays, and random phase fluctuations (Bamler & Hartl, 1998; Lee, Jurkevich, et al., 1994). Such noise adversely affects coherence, which complicates the PSCs identification and subsequent deformation measurements. Consequently, phase filtering techniques are necessary to reduce noise, enhancing the coherence and visibility of stable scatterers (Goldstein & Werner, 1998; Lee et al., 1994). Several known phase filtering methods, including Boxcar (Hanssen, 2001), Goldstein (Goldstein & Werner, 1998), Lee (Lee et al., 1994) and GAMMA (Wegmller et al., 2001) Filters are each characterized by a unique noise mitigation mechanism and trade-offs in preserving spatial details and coherent signals.

This study systematically evaluates the performance of various phase filtering techniques (Boxcar, Goldstein, Lee, and GAMMA) to enhance both spatial and temporal coherence estimations. Using 173 Single Look Complex (SLC) images of Sentinel-1A Ascending Orbit, this research benchmarks the filters' capability in an urban context, especially the Jakarta Capital City of Indonesia. The findings evaluate the strengths and weaknesses in coherence enhancement for PSC selection. Moreover, the result highlights the necessity to improve the PSInSAR accuracy through guiding the optimal phase filtering selection, thus enhancing the reliability of deformation measurement.

Literature Review

PSInSAR has emerged as an essential technique for monitoring long-term surface deformation over urban areas which prone to structural instability and subsidence (Ferretti et al., 2001; Hooper, 2008). PSInSAR exploits stable radar reflectors known as PSCs, which provide reliable phase measurements over extensive observation periods. This technology has seen diverse applications, such as monitoring urban subsidence, landslide detection, infrastructure stability assessments, and monitoring volcanic activity, thus supporting urban planning and risk management.

Despite its strengths, PSInSAR faces significant challenges due to numerous error sources that compromise measurement accuracy. Wu & Madson (2024) categorized these errors into intrinsic height errors, including systematic and random errors, and location-induced errors, such as geometric distortions (shadow, foreshortening, layover). Notably, atmospheric disturbances, orbital inaccuracies, geometric decorrelation, temporal decorrelation, and residual topographic errors are primary contributors to intrinsic height inaccuracies. These error sources significantly influence deformation accuracy, thus highlighting the necessity of advanced error mitigation strategies in PSInSAR measurement.

Effective identification and selection of PSCs critically determine the success of PSInSAR measurements. Phase-based coherence indices, namely Temporal (Hooper et al., 2004) and Spatial Coherence (Zebker & Villasenor, 1992) PSC selection has the capability to support this due to its robustness in quantifying phase stability and consistency. Temporal Coherence assesses individual scattering point stability over time, while Spatial Coherence evaluates phase consistency across neighboring scatterers. However, the absence of direct comparison of these two indices in the same dataset has emerged as one of the motivations of this benchmarking research. Nevertheless, these coherence-based criteria could mitigate errors of the inherent phase signal, leading to improved accuracy and reliability in urban deformation monitoring.

InSAR phase fidelity refers to the ability to preserve the true phase information of the radar signal throughout the processing chain, ensuring that the measured phase remains representative of the actual scattering geometry and displacement (Hanssen, 2001, p. 47). Loss of phase fidelity can arise from inaccurate co-registration, high fringe rates within the estimation window, or topographic distortion, which can bias phase measurements and reduce the reliability of subsequent interferometric products. To maintain phase fidelity, filtering is generally performed on the wrapped interferogram in radar coordinates, where

all phase contributions remain intact, allowing noise suppression while avoiding distortion of the true phase signal.

A posteriori filtering in InSAR is applied after interferogram formation to enhance phase quality by suppressing noise while retaining fringe information. Techniques such as isotropic filters (e.g., Boxcar) and anisotropic or adaptive filters operate in the wrapped interferogram domain, using local spectral properties to selectively reduce noise components perpendicular to the dominant fringe direction (Hanssen, 2001, p.54). By preserving high-frequency phase content along the fringe orientation while reducing incoherent components, these methods maintain phase fidelity and improve unwrapping success, particularly in noisy or heterogeneous terrain.

Several phase filtering methods, notably Boxcar, Goldstein, Lee and GAMMA have been proposed to mitigate the errors. Goldstein filtering selectively enhances coherent signals from stronger scatterers, which is ideal for man-made environments, while Boxcar and GAMMA filtering emphasize on noise reduction and coherent signal preservation over diverse urban-natural settings. Lee filtering dynamically adapts to local noise conditions, thus preserving critical edge details. Therefore, evaluating these filtering would potentially give the contributing insight on the filtering selection over the coastal urban area settings such as Jakarta.

Despite substantial advancements in PSInSAR methodology, persistent issues related to the PSCs density and reliability remains unresolved. Reviews conducted by Alam et al. (2024) and earlier comprehensive systematic literature review by Crosetto et al. (2016) underline the ongoing challenge of achieving dense and reliable PSCs distribution, crucial for precise deformation monitoring. This research addresses the identified gap by systematically benchmarking various phase filtering techniques, specifically within Jakarta's urban environment, to evaluate their efficacy in coherence enhancement for PSC selection. The systematic approach aims to provide robust recommendations on optimal filtering strategies, contributing to enhanced PSInSAR accuracy and reliable urban deformation studies.

Methodology

The methodology employed in this research involves a systematic workflow under The Sentinel Application Platform Graph Processing Tool (SNAP GPT) (European Space Agency, 2024) and Python Processing Environment to assess the effectiveness of different phase indices and filtering techniques for PSCs in PSInSAR. Figure 1 illustrates the

research workflow, outlining PSInSAR processing stages, input data, phase signal processing, main research contribution, research output and future work.

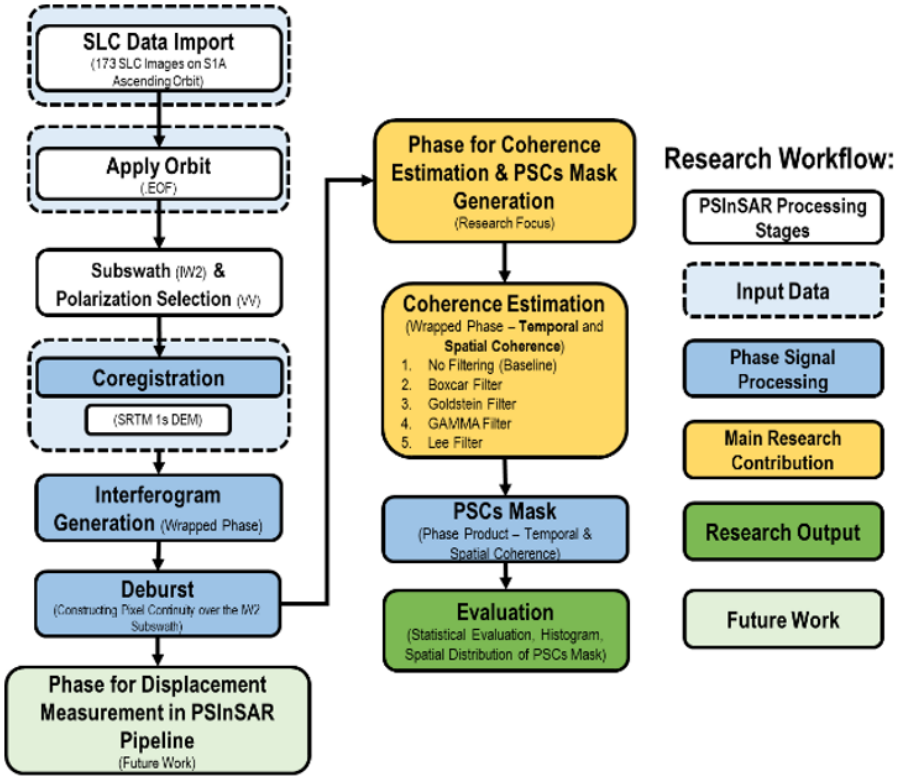

Figure 1: Research Workflow

This study focuses on Jakarta, Indonesia, a densely populated coastal megacity situated on the northwest coast of Java Island. Jakarta lies within a tropical monsoon climate zone and is highly susceptible to land subsidence due to excessive groundwater extraction, rapid urbanization, and soft alluvial deposits. The city's flat topography and extensive built-up areas make it an ideal test site for PSInSAR analysis, particularly for evaluating PSC selection indices.

A total of 173 Sentinel-1A Single Look Complex (SLC) images in ascending orbit geometry were acquired between October 2014 and August 2022. All scenes were captured in Interferometric Wide (IW) swath mode with VV polarization, a nominal incidence angle of ~39, and a 250 km swath width. The dataset covers orbit track 45, ensuring consistent imaging geometry across the study period to minimize baseline decorrelation effects. The Shuttle Radar Topography Mission (SRTM) DEM at 30m spatial resolution, projected to WGS84 was used for topographic phase removal and geocoding purposes.

Data preprocessing up to wrapped interferogram generation and deburst were conducted in SNAP Graph Processing Tool (GPT) environment to ensure a standardized, robust, and reproducible workflow. Steps included precise orbit application, subswath &

polarization selection, coregistration, interferogram generation (wrapped phase), and debursting. A landmask was generated from the DEM and ancillary vector data to exclude water bodies and non-land areas from further analysis. Phase filtering and the computation of Temporal and Spatial Coherence were performed in a Python-based processing environment, offering greater flexibility for implementing custom filtering algorithms and statistical analyses.

To effectively identify optimal PSCs, two essential coherence indices were computed, namely Temporal Coherence (*Yt*) and Spatial Coherence (*Ys*) as explained in Table 1. Temporal Coherence quantifies the phase stability of an individual scatterer over the observation period by considering the standard deviation and median value of wrapped interferograms with values ranging from 0 (unstable) to 1 (stable). Spatial Coherence subsequently computes the consistency of phase signals with neighboring pixels in a 3x3 kernel size, with values spanning from 0 (inconsistent) to 1 (consistent).

Table 1: Phase Indices Used for PSCs Mask Generation

Indices	Formula	Purpose	Value
Temporal Coherence	$\gamma_t = 1 - \frac{\sigma}{\lvert\tilde{\mu}\rvert}$ **Formula Abbreviations:** σ = *standard deviation of phase signal* $\tilde{\mu}$ = *median complex interferometric signal over time*	Compute phase stability over time	0 (unstable) – 1 (stable)
Spatial Coherence	$\gamma_s = \frac{1}{N}\sum_{j=1}^{N} e^{i(\varphi - \varphi_j)}$ **Formula Abbreviations:** φ = *phase of central pixel* φ_j = *phase of neighboring pixel* N = *number of neighbors* e^i = *Euler's formula – convert phase angle into complex unit vector*	Measure phase consistency with neighbors	0 (inconsistent) – 1 (consistent)

Various phase filtering techniques, namely Boxcar, Goldstein, Lee and GAMMA Filtering were applied and compared with the No Filtering as the baseline to measure the effectiveness of each filtering technique. Table 2 summarizes these techniques and their respective mathematical formulas. Boxcar Filtering employs simple spatial averaging of neighboring pixels, effectively reducing random noise at the expense of spatial detail. Goldstein Filtering enhances strong signals, making it ideal for urban settings. Lee filtering dynamically adjusts its smoothing based on local noise conditions, preserving essential image details. GAMMA Filtering applies controlled noise reduction while maintaining significant spatial detail, suitable for mixed urban-natural environments.

Therefore, this comprehensive and systematic methodology enables direct comparison of coherence result under different filtering scenarios, facilitating a robust evaluation of the indices and filtering impact on PSCs selection, thus supporting the accuracy of the subsequent phase deformation measurement.

Table 2: Phase Filtering Techniques for Phase Indices Computation

Technique	Formula	Purpose
No Filtering	Directly compute γ_t and γ_s	a. Used as a reference method without any noise reduction applied b. Help to understand how noisy the original radar data is before any phase filtering is applied
Boxcar	$\gamma_{Boxcar} = \frac{1}{M}\sum_{j=1}^{M}\gamma_j$ **Formula Abbreviations:** *M = number of pixels in the moving window (3 x 3)* *j = pixel inside the window* *$Y_j = e^{i\Phi_j}$; unit phasor at pixel j*	Smooth the radar data by averaging nearby pixels, thus reducing random noise, at the cost of blurring fine details or edges slightly
Goldstein	$\gamma_{Goldstein} = \mathcal{F}^{-1}[\mathcal{F}(e^{i\varphi}).W(f)]$ **Formula Abbreviations:** *F{.}, F^{-1} {.} = 2-D Fourier transform/ inverse Fourier transform* *$e^{i\varphi}$ = complex phasor of phase Φ in radians.* *W (f) = Goldstein weight, with $\alpha = 0.8$; spectral smoothing window = 32x32* *f = (f_x, f_y): 2-D spatial frequency (cycles/ pixel)* *F {$e^{i\varphi}$} = spectrum of the phasor image*	a. Enhances radar signals by focusing more on stronger signals while reducing weaker & noisy signals. b. Ideal for emphasizing strong signals from buildings/ man-made environment
Lee	$FI = \mu + \omega.(I - \mu)$ $\omega = \frac{var}{var + noise\_var}$ $\gamma_{Lee} = \frac{\bar{\gamma}}{1 + \frac{\sigma^2}{\bar{\gamma}^2}}$ **Formula Abbreviations:** *I =$e^{i\varphi}$: input complex phasor at the center pixel* *μ = local mean of I in the window* *var = local variance of I* *noise_var = speckle noise variance, equal to median (var) per tile* *ω = adaptive weight* *FI = filtered complex output* *σ = circular phase variance in the window* *γ = magnitude of the local mean phasor* *N = window size (5x5)*	a. Adjust the filtering strength based on local image conditions. Areas with high noise will have a stronger smoothing effect. b. Excellent for preserving important edges and details while still effectively reducing noise.
GAMMA	$\gamma_{GAMMA} = \mathcal{F}^{-1}[\mathcal{F}(e^{i\varphi}).\exp(-2\pi^2\sigma_x^2\|f\|^2)]$ **Formula Abbreviations:** *F{.}, F^{-1} {.} = 2-D Fourier transform/ inverse Fourier transform* *$e^{i\varphi}$ = complex phasor of the interferometric phase Φ* *f = (f_x, f_y): 2-D spatial frequency (cycles/ pixel)* *σ_x = spatial-domain Gaussian std (cycles/pixel), sigma = 1.0; tiling rows = 1024*	a. Applying a gentle and controlled reduction of noise by removing high-frequency fluctuations without severely blurring the image.

Technique	Formula	Purpose
		b. Offers a balanced result by preserving the important spatial details, effective for mixed urban and natural environments

Results and Discussion

a. Temporal Coherence

The analysis of temporal coherence across different phase filtering scenarios reveals slight variations in spatial distribution, statistical summaries, and histogram characteristics. Spatial distribution maps (Figure 2) and histograms (Figure 3) indicate that GAMMA Filtering produces the highest mean temporal coherence (mean = 0.12), followed closely by Boxcar Filtering (mean = 0.11). Conversely, no filtering results were obtained as the lowest Temporal Coherence values (mean = 0.07). These findings align with the statistical summary presented in Table 3, which further highlights GAMMA and Boxcar Filtering effectiveness in enhancing temporal phase stability by reducing random phase fluctuations.

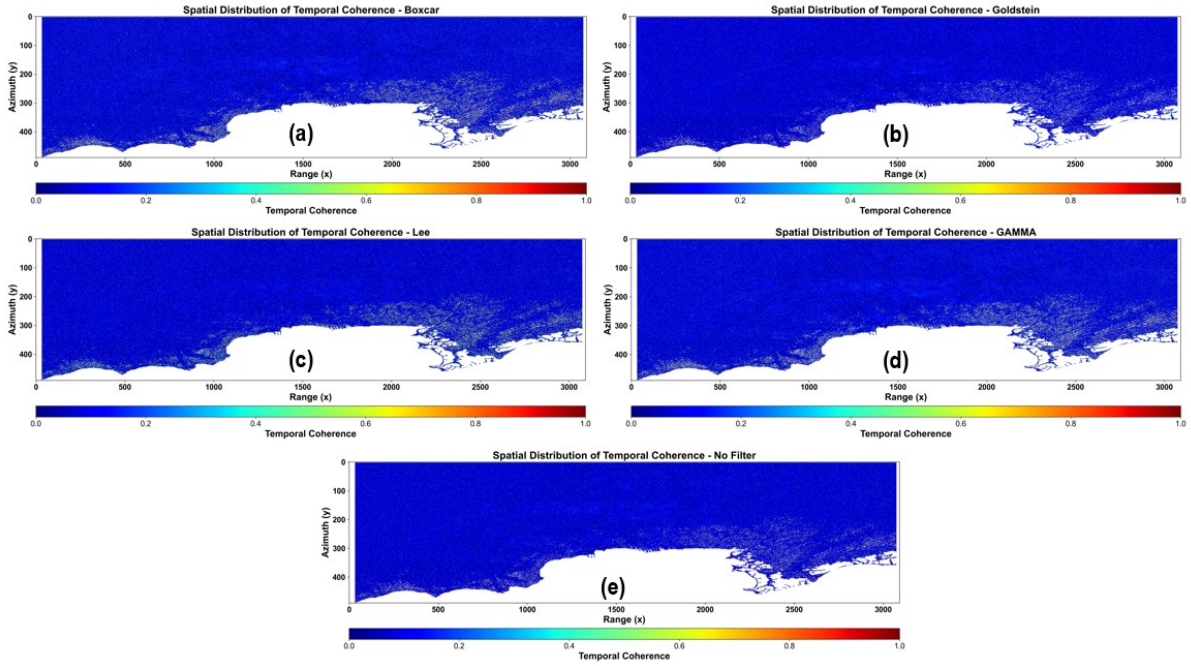

Figure 2: Spatial Distribution of Temporal Coherence for Each Phase Filtering Technique of (a) Boxcar; (b) Goldstein; (c) Lee; (d) GAMMA; and (e) No Filter

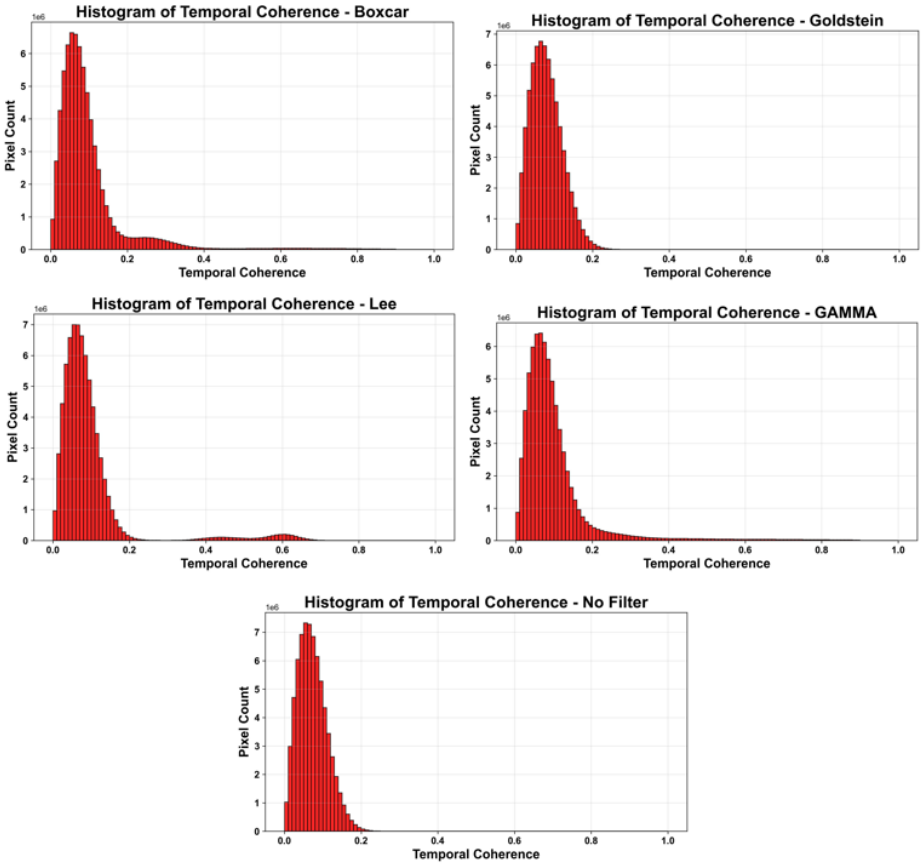

Figure 3: Histogram of Temporal Coherence for Each Phase Filtering Technique

Table 3: Statistical Summary of Temporal Coherence

Filtering Technique	Temporal Coherence Statistical Summary					
	Min	Max	Mean	Median	Std Dev	∑ Pixels
No Filter	0.000	0.365	0.072	0.068	0.037	70.7×10^6
Boxcar	0.000	0.900	0.098	0.074	0.101	72.6×10^6
Goldstein	0.000	0.398	0.079	0.075	0.041	70.7×10^6
Lee	0.000	0.900	0.095	0.072	0.106	72.9×10^6
GAMMA	0.000	0.900	0.100	0.077	0.101	73.3×10^6

b. Spatial Coherence

The measurement of Spatial Coherence exhibits significant enhancement across all phase filtering techniques compared to temporal coherence, as evident from spatial distribution maps (Figure 4) and corresponding histograms (Figure 5). GAMMA Filtering yields the highest Spatial Coherence (mean = 0.76), demonstrating its superior capability to suppress speckle noise while preserving coherent urban signals. Subsequently, Boxcar Filtering similarly shows high Spatial Coherence (mean = 0.72) with slightly compromised spatial detail. In contrast, Goldstein (mean = 0.43) and Lee Filtering (mean = 0.47) provide moderate improvements, with significantly lower coherence than GAMMA and Boxcar Filtering, as shown in Table 4.

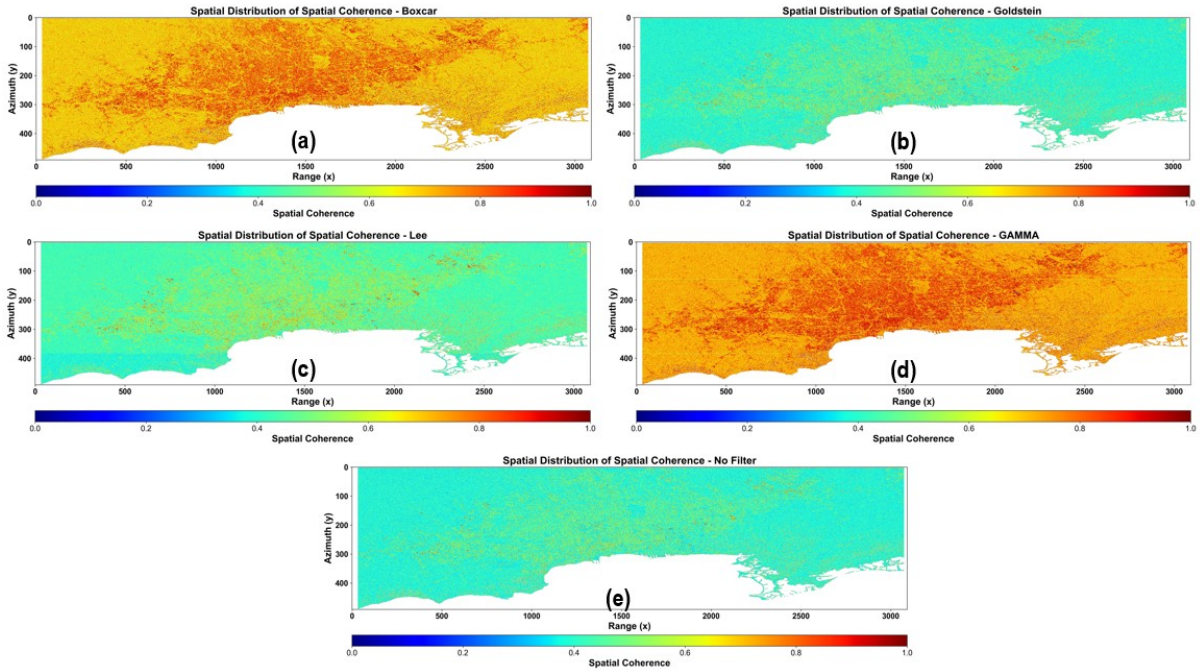

Figure 4: Spatial Distribution of Spatial Coherence for Each Phase Filtering Technique of (a) Boxcar; (b) Goldstein; (c) Lee; (d) GAMMA; and (e) No Filter

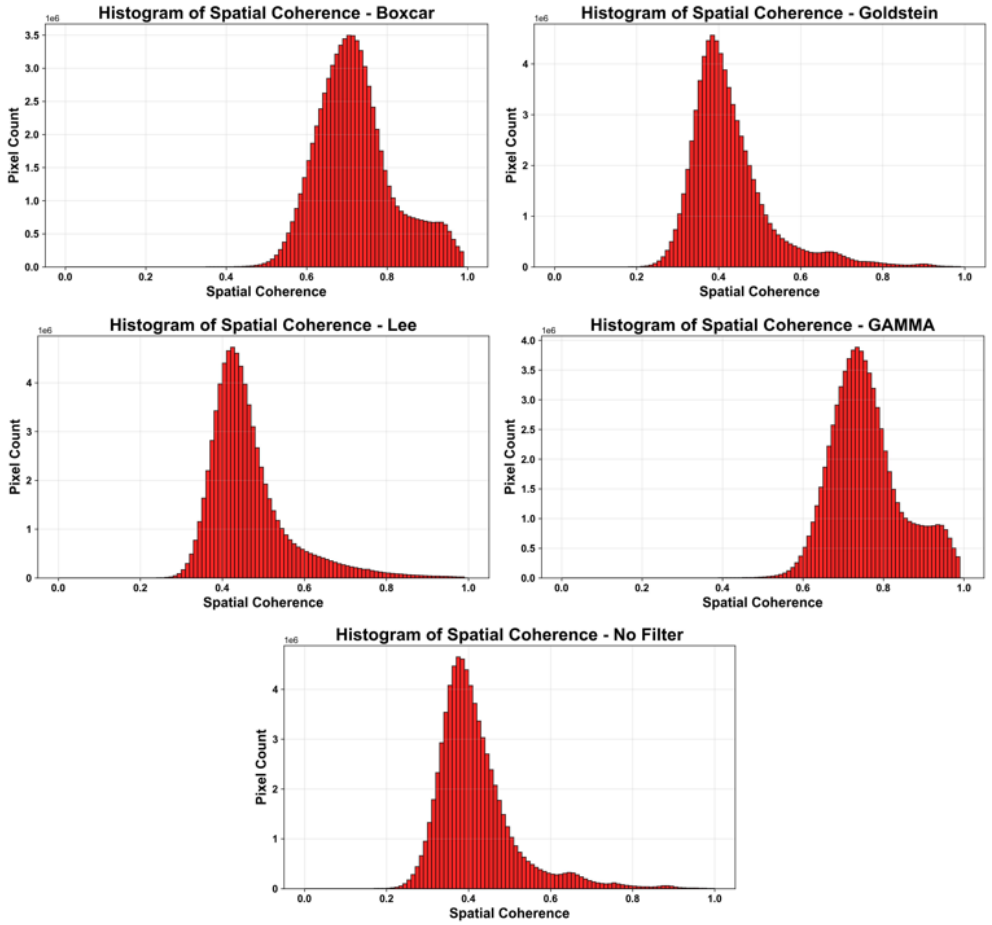

Figure 5: Histogram of Spatial Coherence for Each Phase Filtering Technique

Table 4: Statistical Summary of Spatial Coherence

Filtering Technique	Spatial Coherence Statistical Summary					
	Min	Max	Mean	Median	Std Dev	∑ Pixels
No Filter	0.054	0.997	0.418	0.398	0.096	72.6×10^6
Boxcar	0.121	0.998	0.723	0.712	0.097	73.0×10^6
Goldstein	0.051	0.990	0.428	0.407	0.099	72.6×10^6
Lee	0.098	0.990	0.464	0.442	0.098	73.1×10^6
GAMMA	0.145	0.990	0.758	0.746	0.088	73.4×10^6

Although GAMMA yields the highest mean spatial coherence, the applied tile-based spectral filtering introduced horizontal seams at tile boundaries, which locally inflate coherence along these rows. In comparison, Boxcar Filtering, despite slightly producing lower mean coherence, does not exhibit such pronounced systematic artifacts, potentially providing more reliable and artifact-free PSC selection.

c. Defining the Effective Phase Filtering and Indices for PSCs

The comparative evaluation clearly indicates that spatial coherence is more effective for PSCs selection than temporal coherence. Spatial Coherence measures consistency with neighboring pixels, providing a robust index that accounts for local phase variations, while Temporal Coherence assesses individual pixel stability over time, making it inherently stricter and sensitive to noise (Osmanoglu et al, 2016; Werner, 2003). Spatial Coherence inherently incorporates redundancy by averaging across neighboring pixels, making it less susceptible to individual pixel noise fluctuations and thus better suited for reliable PSC selection, especially in the heterogeneous urban environments of Jakarta, the Capital City of Indonesia.

d. Discussion

Phase filtering is theoretically validated to be conducted exclusively on wrapped interferograms to preserve phase fidelity, ensuring that all phase contributions (topographic, flat-earth, atmospheric, and orbital components) remain intact (Hanssen, 2001; Zebker & Villasenor, 1992). Filtering post-unwrapping, conversion from radar coordinate to geographic coordinate, or after removal of phase contribution, may introduce errors by breaking the fundamental phase relationships and leading to coherence overestimation (Goldstein & Werner, 1998). Retaining the wrapped phase data in radar coordinates ensures accurate and faithful representation of actual phase relationships, essential for precise deformation analysis.

In this study, the superior performance of Spatial Coherence over Temporal Coherence can be linked to the preservation of phase fidelity. Spatial Coherence, calculated

in the wrapped interferogram domain, operates on neighborhood-based phase similarity, inherently retaining the complete phase contributions and thus aligning with the theoretical requirement for fidelity preservation (Hanssen, 2001, p.47). Temporal Coherence, in contrast, involves pixel-wise correlation over time and can degrade when computed on unwrapped or corrected interferograms, where certain phase contributions (e.g., topography, orbital ramps, atmosphere) have been removed. This results in an underestimation of coherence in areas with subtle deformation signals. Temporal Coherence can perform optimally when computed on long, high-quality time series with minimal decorrelation sources and when phase is preserved in its wrapped state prior to any unwrapping.

Furthermore, the widely accepted coherence threshold for PSC selection in PSInSAR typically ranges between 0.3 to 0.6, depending on the application and urban context (Ferretti et al., 2001; Hooper et al., 2004). Our results demonstrate that the spatial coherence, particularly using GAMMA and Boxcar Filtering methods, surpasses these thresholds, validating its practical utility for PSC selection in urban deformation monitoring. This research clearly underscores the superiority of Spatial Coherence indices and GAMMA Filtering techniques, reinforcing their applicability and recommending their use in urban PSInSAR studies.

Urban environments like Jakarta are characterized by dense distributions of artificial corner reflectors such as building edges, rooftops, and metallic structures, which naturally sustain high Spatial Coherence. The neighborhood-based nature of Spatial Coherence calculation allows it to tolerate minor local phase disturbances by averaging over surrounding pixels, preserving stability even in rural areas undergoing small-scale changes. In contrast, Temporal Coherence, which is calculated on a pixel-wise basis, retains any decorrelation from surface changes or atmospheric variability. Jakarta's periodic flooding and construction activities introduce significant temporal phase instability, leading to lower temporal coherence values despite high spatial stability. These factors collectively explain why Spatial Coherence consistently outperforms Temporal Coherence in this study, particularly in built-up urban settings where the scatterer's consistency outweighs its stability over long time intervals. Subsequently, in terms of the accuracy of the surface deformation measurement from each index, it has yet to be presented in this study; thus, it is considered part of the future work's content.

The application of a posteriori filtering in this study, particularly GAMMA and Boxcar, follows the principle outlined by Hanssen (2001, p.54) in which filtering is

performed on the wrapped interferogram to balance noise suppression and fringe preservation. Operating in the spectral domain allows these filters to enhance coherent phase signals without distorting the underlying deformation pattern, a key factor in maintaining phase fidelity. This aligns with our findings, where wrapped-domain filtering not only elevated Spatial Coherence beyond commonly accepted PSC thresholds, but also ensured the retention of fine-scale fringe structures necessary for accurate displacement retrieval in urban PSInSAR measurement.

Regarding the horizontal line artifacts produced from GAMMA Filtering, several notable mitigation strategies include Pixel Averaging, Threshold-Based Pixel Masking, or Increased Neighborhood Size. Pixel Averaging means applying the average along the affected rows to reduce the presence of artifacts, thus preserving the integrity of Spatial Coherence. Moreover, Threshold-Based Pixel Masking is to explicitly mask out entire rows with unrealistic coherence values, especially if coherence is persistently close to saturation (> 0.90 to 1). Subsequently, Increased Neighborhood Size means to expand the Spatial Coherence Window from the prior 3x3 to 5x5 or higher, thus reducing the visibility of linear artifacts.

Conclusion and Recommendation

This research systematically evaluated phase filtering and indices for coherence enhancement and Persistent Scatterer Candidates (PSCs) selection in PSInSAR measurement. Our findings demonstrate the superiority of Spatial Coherence indices over Temporal Coherence for effectively identifying PSCs in urban environments. Spatial Coherence, particularly when computed using GAMMA and Boxcar Filtering methods, significantly surpasses conventional coherence thresholds (0.3 – 0.6), providing robust and reliable PSC selection necessary for accurate space-borne deformation measurement.

Among the evaluated phase filtering techniques, GAMMA filtering consistently delivered the highest spatial coherence, offering the most effective noise suppression while maintaining critical spatial details necessary for precise deformation analysis. Boxcar filtering also showed commendable performance. Conversely, Goldstein and Lee Filtering offers some improvement but was less effective in coherence enhancement compared to GAMMA and Boxcar approaches. From a methodological perspective, our results reinforce the theoretical importance of applying phase filtering exclusively to wrapped interferograms, preserving phase fidelity and preventing coherence overestimation. This approach is crucial for maintaining accurate phase relationships required for reliable deformation analysis.

Although GAMMA Filtering consistently produced the highest coherence values, the presence of systematic horizontal artifacts reveals a notable limitation. Consequently, Boxcar Filtering may offer a more reliable alternative by avoiding such artifacts and ensuring consistently trustworthy coherence values. We recommend further evaluation of filtering-window strategies or explicit row-wise pixel averaging to mitigate identified GAMMA filtering artifacts for future PSInSAR applications.

The demonstrated superiority of Spatial Coherence for PSC selection in Jakarta suggests that the future PSInSAR measurement framework in similar coastal megacities should prioritize neighborhood-based indices. This finding, however, is yet to be tested for its performance in terms of accuracy from the derived surface deformation measurement, which aligns with the future work's content. Additionally, this approach can be readily scaled to other urban environments with comparable scatterer distributions, enabling more robust deformation monitoring despite dynamic land cover changes or challenging climatic conditions.

References

Alam, M. S., Kumar, D., & Vishwakarma, G. K. (2024). A review on advances in persistent scatterer interferometry and proposing a novel method for phase optimization of distributed scatterers pixels. *Journal of Engineering Mathematics*, *145*(1). https://doi.org/10.1007/s10665-024-10354-2

Bamler, R., & Hartl, P. (1998). Synthetic aperture radar interferometry. *Inverse Problems*, *14*(4), R1–R54. https://doi.org/10.1088/0266-5611/14/4/001

Crosetto, M., Monserrat, O., Cuevas-González, M., Devanthéry, N., & Crippa, B. (2016). Persistent Scatterer Interferometry: A review. *ISPRS Journal of Photogrammetry and Remote Sensing*, *115*, 78–89. https://doi.org/https://doi.org/10.1016/j.isprsjprs.2015.10.011

European Space Agency. (2024). *SNAP—Sentinel Application Platform* .

Ferretti, A., Prati, C., & Rocca, F. (2001). Permanent scatterers in SAR interferometry. *IEEE Transactions on Geoscience and Remote Sensing*, *39*(1), 8–20. https://doi.org/10.1109/36.898661

Goldstein, R. M., & Werner, C. L. (1998). Radar interferogram filtering for geophysical applications. *Geophysical Research Letters*, *25*(21), 4035–4038. https://doi.org/https://doi.org/10.1029/1998GL900033

Hanssen, R. F. (2001). *Radar Interferometry* (2nd ed.). Springer Netherlands. https://doi.org/10.1007/0-306-47633-9

Hooper, A. (2008). A multi-temporal InSAR method incorporating both persistent scatterer and small baseline approaches. *Geophysical Research Letters*, *35*(16). https://doi.org/https://doi.org/10.1029/2008GL034654

Hooper, A., Zebker, H., Segall, P., & Kampes, B. (2004). A new method for measuring deformation on volcanoes and other natural terrains using InSAR persistent scatterers. *Geophysical Research Letters*, *31*(23). https://doi.org/https://doi.org/10.1029/2004GL021737

Lee, J. S., Hoppel, K. W., Mango, S. A., & Miller, A. R. (1994). Intensity and phase statistics of multilook polarimetric and interferometric SAR imagery. *IEEE Transactions on Geoscience and Remote Sensing*, *32*(5), 1017–1028. https://doi.org/10.1109/36.312890

Lee, J. S., Jurkevich, L., Dewaele, P., Wambacq, P., & Oosterlinck, A. (1994). Speckle filtering of synthetic aperture radar images: A review. *Remote Sensing Reviews*, *8*(4), 313–340. https://doi.org/10.1080/02757259409532206

Wegmller, U., Strozzi, T., & Wiesmann, A. (2001). GAMMA SAR and interferometric processing software. *Proceedings of the ERS-Envisat Symposium*.

Wu, Y. Y., & Madson, A. (2024). Error Sources of Interferometric Synthetic Aperture Radar Satellites. In *Remote Sensing* (Vol. 16, Issue 2). Multidisciplinary Digital Publishing Institute (MDPI). https://doi.org/10.3390/rs16020354

Zebker, H. A., & Villasenor, J. (1992). Decorrelation in interferometric radar echoes. *IEEE Transactions on Geoscience and Remote Sensing*, *30*(5), 950–959. https://doi.org/10.1109/36.175330